GROUND MOTION MEASUREMENTS IN A HERA INTERACTION REGION

C. Montag, DESY

Abstract

Ground motion is of great importance for the performance of any future Linear Collider, because it is a possible source of severe luminosity degradation. To estimate the expected detrimental effects and to define the requirements for feedback systems, it is necessary to understand vibration properties in an accelerator tunnel and especially in the interaction region. Therefore the HERA electron-proton collider has been taken as a realistic invironment to study ground motion.

1 INTRODUCTION

To achieve the high design luminosity of some $10^{34}\,\mathrm{cm}^{-2}\mathrm{sec}^{-1}$, all Linear Collider schemes under study require extremely low emittance beams focused to spot sizes of about $\sigma_x = 100\,\mathrm{nm}$ width and $\sigma_y = 10\,\mathrm{nm}$ height at the interaction point (IP). Since ground motion effects in the entire linac lead to beam orbit vibrations, it is necessary to compensate beam jitter at the IP by some kind of feedback system. In the case of TESLA, a fast bunch-to-bunch feedback system based on the beam-beam interaction is foreseen [1]. While this feedback system is able to compensate an initial relative beam offset of $100\,\sigma_y$ within $3\,\%$ of the bunch train consisting of 2820 bunches, it would nevertheless be desirable to set-up the machine in a single bunch mode. This scheme defines the tolerances for quadrupole motion in the entire machine, leading to beam jitter, as well as for the relative vibration of the final beam position monitors (BPMs) used for beam steering at the IP.

To estimate the amplitudes of relative motion of the final BPMs with respect to each other that have to be expected in a real interaction region environment, the motion of the two tunnel ends at HERA Hall East has been studied. Figure 1 shows schematically the geometry and various measurement points as referred to in the rest of this paper.

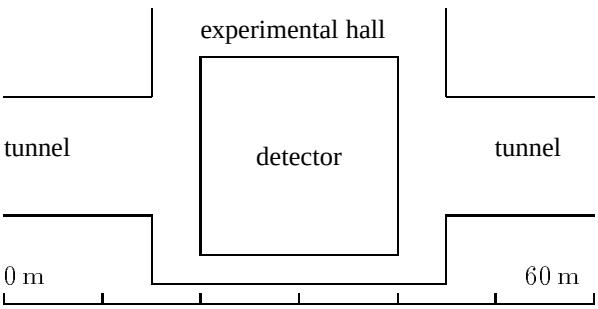

Figure 1: Schematic side view of HERA Hall East with the detector and the accelerator tunnel ends.

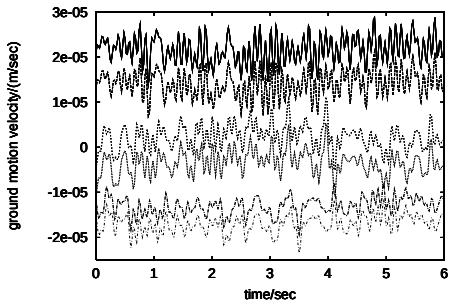

Figure 2: Primary velocity output signals of the two seismometers when placed side-by-side. The two upper lines show the signals of the two vertical sensors, the 3rd and 4th curve corresponds to the motion in one transverse ("North-South") direction, while the two lower lines show the signals in the perpendicular direction ("East-West"). In order to get clearly distinguishable lines in this plot, some offset has been added to each signal here.

2 INSTRUMENTATION

All measurements were performed with three-axis GURALP CMG-3 seismometers [2], having a flat transfer function from $2.8 \cdot 10^{-3}\,\mathrm{Hz}$ to $50\,\mathrm{Hz}$. These instruments are equipped with 16-bit ADCs attached directly to the seismometers, thus providing noise-free digital signal transfer. The sensitivity of these instruments can be selected remotely via a PC from $2.3\,\mathrm{nm\,sec}^{-1}/\mathrm{bit}$ to $300\,\mathrm{nmsec}^{-1}/\mathrm{bit}$. During all measurements the highest sensitivity was used.

While the primary sampling rate of the ADC is $2\,\mathrm{kHz}$, this is reduced by means of digital filters to an output rate of $50\,\mathrm{Hz}$. The cutoff frequency of the digital lowpass filter can be set remotely to 5, 10, or 20 Hz, respectively.

To confirm the high signal-to-noise ratio of these instruments, both seismometers were placed side-by-side, and the output data of both instruments were recorded within a time interval of $2\,1/2\,\mathrm{hours}$. Figure 2 shows an example of the primary sensor signals. As figure 2 shows, the output signals of both seismometers agree nicely with each other. To quantify this, the coherence function

$$|\gamma| = \frac{|\langle X_1 X_2^* \rangle|}{\sqrt{\langle X_1 X_1^* \rangle \langle X_2 X_2^* \rangle}}, \qquad (1)$$

where $X_1 = X_1(\omega)$, $X_2 = X_2(\omega)$ are the respective Fourier transforms of the time domain signals $x_1(t)$, $x_2(t)$, has been calculated. Here the asterisk indicates the complex conjugate, while the brackets $\langle \ldots \rangle$ mean averaging over different data samples. Figure 3 shows the resulting

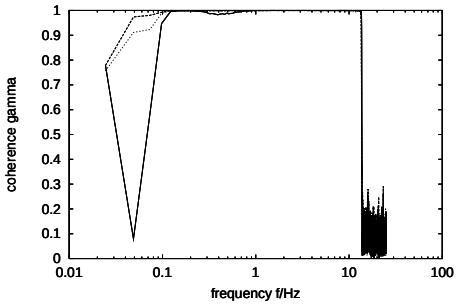

Figure 3: Coherence functions $|\gamma(\omega)|$ in all three directions for the sensors placed side-by-side.

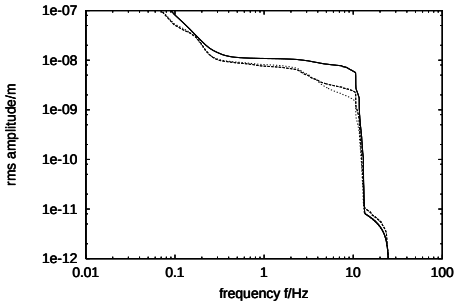

Figure 4: rms value of the difference signal of each pair of corresponding sensors placed side-by-side. In the vertical direction (upper, solid line), the rms difference signal is significantly larger than in the two horizontal directions.

coherence in the case of the sensors being placed side-by-side. In all three directions, the coherence is very close to unity in the frequency range from $0.1\,\mathrm{Hz}$ to $12\,\mathrm{Hz}$, though no thermal insulation etc. was applied.

Using the power spectrum $\Phi_{x_1-x_2}(\omega) = \langle (X_1(\omega) - X_2(\omega)(X_1(\omega) - X_2(\omega))^* \rangle$, the rms value $\sigma_{x_1-x_2}$ in the frequency band from f_1 to f_2 can be calculated as

$$\sigma_{x_1-x_2} = \sqrt{\int_{2\pi f_1}^{2\pi f_2} \Phi_{x_1-x_2}(\omega)\,\mathrm{d}\omega}\,. \qquad (2)$$

Figure 4 shows the resulting rms difference signal in the frequency band from f_0 to $25\,\mathrm{Hz}$ (the cutoff frequency of these instruments) as a function of the lower frequency limit f_0.

Below roughly $0.1\,\mathrm{Hz}$, the output signals are obviously dominated by internal noise of the seismometers, while above that limit both probers agree within $10\,\mathrm{nm}$.

3 MEASUREMENTS

After the performance of the seismometers had been checked as described above, they were placed in the HERA tunnel around the interaction region (Hall West). The locations of the seismometers and the resulting distances between them during the measurements are given in table 1.

loc. sensor 1	loc. sensor 2	distance/m
OL17	OR17	34
OL17	OR34	51
OL30	OR34	64

Table 1: Locations and distances of sensors used during the experiments."R" and "L" stand for "right" and "left" of the interaction point as seen from the center of the HERA accelerator ring, respectively, while the numbers indicate the respective distances in meters from the interaction point.

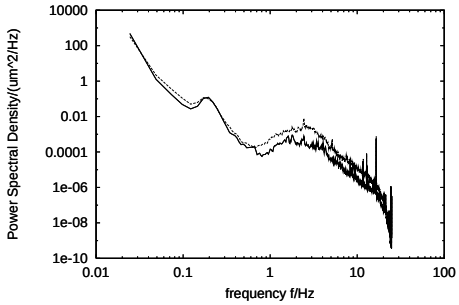

Figure 5: Vertical ground motion spectra obtained in a single point under quiet conditions during the night (solid line) and during the rush hour (dashed curve).

After the sensors had been installed and were properly centered, data were recorded continuously for 12 hours with each configuration, always starting at about 9:00 p. m. in order to keep the influence of traffic on a nearby main road and other human activities similar for all measurements. As an example, figure 5 shows ground motion spectra obtained in a single point during the quiet time from 2:00 a. m. to 3:00 a. m. and during the rush hour from 8:00 a. m. to 9:00 a. m. Figure 6 shows the corresponding rms ground motion amplitude in the frequency band from f_0 to $25\,\mathrm{Hz}$ as a function of the lower frequency limit f_0, calculated from these spectra. As mentioned earlier, the relative motion of the two tunnel ends around the interaction region with respect to each other is of particular interest for Linear Collider design and performance. Therefore the difference of the signals of corresponding sensors on both sides of the interaction point was calculated. The lower part of figure 6 shows the rms relative vertical motion amplitude in the frequency band from f_0 to $25\,\mathrm{Hz}$ as function of the lower frequency limit f_0 for a distance of $34\,\mathrm{m}$ under quiet and noisy conditions. Compared to the corresponding data in a single point (upper part of figure 6), the rms amplitude of the relative motion of the two tunnel ends for frequencies f_0 above some $1\,\mathrm{Hz}$ is approximately equal to the rms amplitude in a single point, while for frequencies f_0 below $1\,\mathrm{Hz}$ the relative motion is smaller compared to the rms amplitudes in a single point. In the case of completely incoherent motion of the two points, the rms value of the relative motion would be a factor $\sqrt{2}$ larger than the corre-

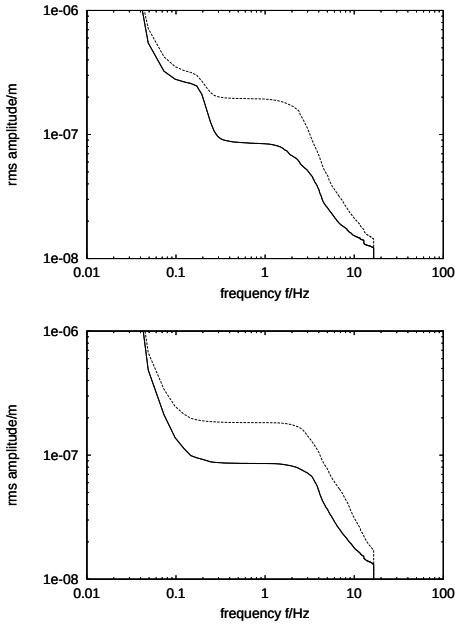

Figure 6: rms vertical ground motion amplitudes in the frequency band from f_0 to $25\,\mathrm{Hz}$ as a function of the lower frequency limit f_0 under quiet (solid line) and noisy conditions (dashed curve). The upper plot shows the rms value in a single point as calculated from the spectra shown in figure 5. In the lower plot, the rms value of the relative motion of the two tunnel ends over a distance of $34\,\mathrm{m}$ is given.

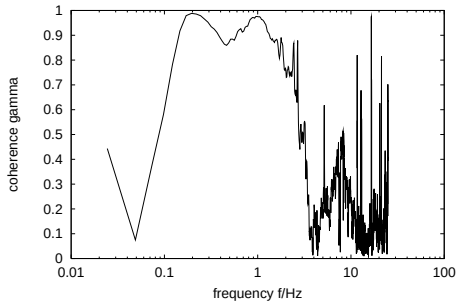

Figure 7: Coherence $|\gamma|$ of the vertical motion of the two tunnel ends over a distance of $34\,\mathrm{m}$.

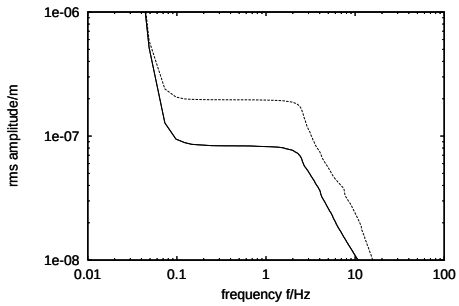

Figure 8: rms amplitudes of the relative horizontal motion of the two tunnel ends over a distance of $34\,\mathrm{m}$ under quiet (solid line) and noisy conditions (dashed line).

sponding value in a single point. The so-called microseimic peak around $0.14\,\mathrm{Hz}$ vanishes in the difference signal due to the very good coherence and long wavelength.
This behaviour is reflected in the coherence function, figure 7, showing that the vertical motion of both sides is practically uncorrelated at frequencies above about $2\,\mathrm{Hz}$, while below that frequency the coherence is close to unity. The bad coherence at very small frequencies below some $0.1\,\mathrm{Hz}$ can be explained by the lack of any thermal insulation of the sensors during the measurements.

At larger distances (see table 1), the coherence $|\gamma|$ drops at slightly lower frequencies of about $1\,\mathrm{Hz}$, but in terms of rms vibration amplitudes of the relative motion of the two locations, the result does not show any significant differences compared to the case at $34\,\mathrm{m}$ distance.
The ground motion data obtained in the horizontal direction perpendicular to the beam direction are very similar to the vertical motion, see figure 8.

4 CONCLUSION

As a rule of thumb, a displacement Δx, Δy of the final quadrupoles in the interaction region of a linear collider translates to roughly the same orbit displacement at the interaction point. In the case of TESLA, the final doublets will be some $10\,\mathrm{m}$ apart. Therefore the measurements presented in this paper provide an upper limit of the relative motion to be expected for these magnets, but it is unlikely that the situation will be much more relaxed. Since the vertical motion of both tunnel ends in the interaction region is practically uncorrelated for frequencies above some $3\,\mathrm{Hz}$ and exceeds the vertical beam size by far, some means of active stabilization [3] will certainly be necessary to obtain collisions in the single bunch mode, even if the low-β optics is somewhat relaxed compared to the nominal operation with long bunch trains.

5 ACKNOWLEDGEMENTS

The author would like to thank S. Herb for help with the HERA network environment, and R. Brinkmann for helpful discussions.

REFERENCES

[1] I. Reyzl, Stabilization of Beam Interaction in the TESLA Linear Collider, these proceedings

[2] CMG-3T operation manual, Guralp Systems Ltd., Aldermaston 1993

[3] C. Montag, Active Stabilization of Mechanical Quadrupole Vibrations for Linear Colliders, Nucl. Instr. Meth. A 378 (1996), 369-375